Micellar Solutions of Associative Triblock Copolymers: The Relationship between Structure and Rheology

Q. T. Pham† and W. B. Russel*

Department of Chemical Engineering, Princeton University, Princeton, New Jersey 08544

J. C. Thibeault and W. Lau

Research Laboratories, Rohm and Haas Company, Spring House, Pennsylvania 19477

Received February 17, 1999; Revised Manuscript Received May 4, 1999

ABSTRACT: We report the rheology of the micellar solutions formed from narrow-molecular-weight poly(ethylene oxide) chains fully endcapped with C_{16} or C_{18} alkanes and correlate the viscoelasticity, characterized by the high-frequency modulus G_∞' and a single relaxation time λ, with the measured characteristics of the micellar solutions. Scaling G_∞' by $p^{3/2}kT/\tau R_H^3$ (p = aggregation number, R_H = hydrodynamic radius, $1/\tau$ = attractive virial coefficient, k = Boltzmann's constant, and T = temperature) and plotting against the hydrodynamic volume fraction of micelles collapses the two sets of data. The relaxation time scales as the diffusion time, $\mu R_c^3/kT$, for a free hydrophobe escaping from a micellar core of radius R_c times a Boltzmann factor accounting for an association energy that increases linearly with hydrophobe length. The low shear viscosity follows as $\eta_o = \lambda G_\infty'$.

1. Introduction

A number of groups have described in detail the association[1−4] and rheology[5−9] of aqueous solutions of hydrophobically modified poly(ethylene oxide)s (PEOs) with a range of backbone molecular weights and hydrophobe sizes. This work identifies backbones of intermediate molecular weights, e.g., 35 kg/mol, with C_{12}−C_{16} hydrophobes as producing highly viscous solutions with simple viscoelastic behavior. Our previous paper[10] characterized the micellization of a model associative triblock or telechelic copolymer consisting of a PEO backbone of 35 kg/mol molecular weight with C_{16} and C_{18} terminal groups attached via urethane (isocyanate) coupling groups.

In dilute solutions, these associative polymers form micelles of radius R (∼20 nm) above a rather low critical micellar concentration ($c_{cmc} \ll 0.1$ wt %) that depends on the backbone molecular weight and the hydrophobe size.[1,2,4] The aggregation numbers p vary from 10 to 80, depending on the molecular structure and method of measurement.[10] For isolated micelles, the star polymer model of Daoud and Cotton[11] captures the relation between micelle size and aggregation number. Associating micelles can be viewed to first order as adhesive hard spheres with an interaction strength $1/\tau$ that depends on p and R, although the repulsion is actually softer and the attraction of longer range. The attraction was recognized by Semenov et al.[12] on the basis of earlier theory by Milner and Witten[13] to be entropic in origin, with an energy of 1 kT per chain in the gap (k = Boltzmann's constant, T = absolute temperature) and a range equivalent to the outermost blob size. Hence, when micelles in dilute solution interact, a few bridging chains suffice to account for the nonidealities deduced from experiments. The resulting phase diagram (Figure 1) expressed in terms of the interaction strength $1/\tau$ and the hydrodynamic volume fraction ϕ identifies the gas- and liquid-phase boundaries for the PEO with C_{16} (HDU) and C_{18} (ODU) hydrophobes. A percolation transition extends upward from the critical point, placing the condensed liquid phase well within the percolated regime.

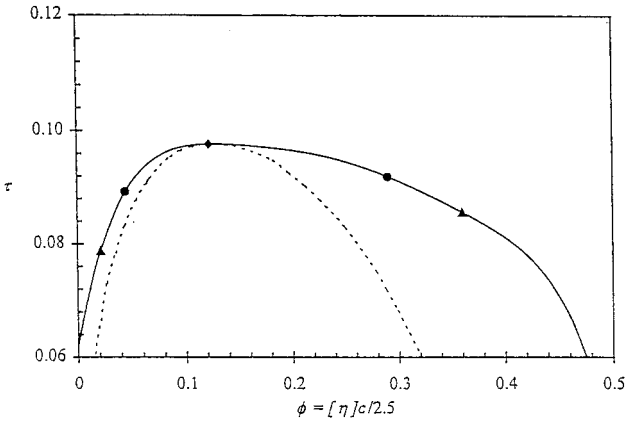

Figure 1. Adhesive hard sphere phase diagram showing the binodal (—), the spinodal (- - -), and the critical point (◆) with the coexisting concentrations for HDU (●) and ODU (▲) superimposed onto the binodal (from ref 10 with permission).

With increasing concentration, the viscosity rises dramatically, well above that of comparable PEO solutions, providing convincing evidence of a high degree of association. The solutions generally exhibit an extended low shear plateau (to shear rates > 100 s^{-1}) with a modest degree of shear thickening (less than a factor of 2) followed by rather dramatic shear thinning. The linear viscoelastic response is beautifully simple with a single relaxation time of $O(10^{-2}$ s) that varies exponentially with the size of the hydrophobe but only modestly with concentration, even with polydisperse backbones. Binary mixtures with the same backbone molecular weight but different hydrophobes display two distinct relaxation times.[7] Although the dependence of the behavior on molecular structure, as well as surfactant and cosolvent concentration, is qualitatively clear, detailed comparisons are confounded by polydispersity

† Current address: Unilever Research, Edgewater, NJ.

10.1021/ma990215x CCC: $18.00
Published on Web 06/29/1999

of the backbone, incomplete capping with the hydrophobes, and (to a lesser extent) internal hydrophobes between PEO blocks.

Thus far, the interpretation of the rheological behavior has depended on the reversible network theory, effectively ignoring the observations of micelle formation at dilute concentrations. This approach succeeds qualitatively, since the shear viscosity is clearly controlled by dissociation of the hydrophobe from a junction or hydrophobe. Capturing the concentration dependence, which derives from the high-frequency modulus for a fluid with a single relaxation time, is more difficult. Statistical analyses that modify the classical theory to allow for loops and junctions of modest and variable size can correlate the observations[7] but overlook the physics of micellization and the rather large aggregation numbers detected.[1,10] More recent theory for flowerlike micelles formed by associative polymers[12] offers a sounder basis by accounting for the entropic attraction that makes bridging favorable and causes the degree of association to increase with concentration. Presumably, the structure and behavior reach the transient network limit when all chains form bridges and excluded volume interactions are fully screened. At intermediate concentrations, the dissociation/association kinetics of the hydrophobe can control the viscosity, but the modulus depends on the interaction potential between micelles, which includes excluded volume effects.

Our objective here is to report the rheology of the micellar solutions formed from narrow-molecular-weight PEO chains fully endcapped with C_{16} or C_{18} alkanes and correlate the viscoelasticity with the measured characteristics of the micellar solutions. These ideal systems reveal novel behavior that motivates a different interpretation of well-established features of the phenomena. The previous paper[10] established the strength of the attraction as well as the size and aggregation number of the micelles from measurements of the low shear viscosity and diffusion coefficient for the dilute micellar phase. This paper demonstrates that the dependence of the shear modulus on concentration and aggregation number resembles that of colloidal dispersions with soft repulsive potentials more than the expectations from the reversible network theory. Consequently, we draw on the adhesive hard sphere model and the earlier characterization of the micellar structure and interactions to interpret the measurements. Finally, the relaxation time appears to scale with the diffusion time of the hydrophobe escaping the micelle, independent of the relaxation of the rest of the chain, providing the sole remaining link with the reversible network theory. These results comprise the first true structure−property relations for this class of associative polymers.

2. Theoretical Background

Associative polymers form viscoelastic fluids with binding energies that control the rate at which chain ends disengage to permit flow. First formalized by Green and Tobolsky,[14] the transient network theory assumes either a θ solvent or a concentrated solution of elastically effective chains at number density n that form a homogeneous network. The theory predicts a high-frequency modulus that derives entirely from the entropic elasticity of the bridging chains and varies linearly with concentration,

$$G_\infty' = nkT \tag{1}$$

with $n = cN_A/M$, where c is the concentration of fully endcapped chains of molecular weight M and N_A is Avogadro's number. The low shear viscosity is then

$$\eta_o = \lambda G_\infty' \tag{2}$$

with the single relaxation time, λ, controlled by the dissociation of the hydrophobe from a junction,

$$\lambda = \frac{s^2}{D_s} e^{\chi} \tag{3}$$

with some characteristic length s, association energy χ, diffusion coefficient $D_s \approx kT/3\pi\mu s$, and solvent viscosity μ. Recent elaborations of the transient network theory account for non-Newtonian behavior and more complex concentration dependence via breakage functions for the junctions, nonaffine deformation, and statistical descriptions of the chain configurations.[5,7,15] Annable et al.,[7] for example, developed a statistical model to relate the nonlinear concentration dependence of η_o and G_∞' to the network topology. They reported good quantitative fits with experimental data but deduced the junction functionality, i.e., aggregation number, to be less than 10, which clearly conflicts with much of the data.

Alternatively, Semenov et al.[12] adapted the Daoud−Cotton model for star polymers and diblock micelles to triblock copolymer brushes in a good solvent. This model treats each half of a triblock in a micelle containing $p \gg 1$ chains with $2N$ segments per midblock, for example, as a radial string of blobs that fill space. The nominal radius of the micelle, $R = 1.172p^{1/5}s$ (s = end-to-end distance for half the midblock), then equals the distance to the outer edge of the outermost blob, which has diameter ξ_o. Since all ends are assumed to reside at the outer edge, $\xi_o = (4\pi/p)^{1/2}R$. The corresponding segment density decays algebraically with radial position and then drops discontinuously to zero at $r = R$. Of course, the latter is unphysical and the authors noted that the segment density should tend to zero exponentially for $r - R \gg \xi_o$. In addition, a spatial distribution of the ends might affect the profile for $R - r \ll \xi_o$. Their correction, based on detailed results for planar brushes, predicts somewhat larger blobs at the outer edge. We have not adopted this correction, since the analysis of Li and Witten[16] for spherical micelles indicates that all ends should lie in the outermost blob for $6 < p < 1600$, which covers the range of interest to us.

For $\chi \gg 1$ such that endblocks are rarely found outside the micellar core, they constructed an interaction potential consisting of (i) a core of radius R and "softness" ξ_o (the compression associated with kT of energy) and (ii) an entropic attraction due to exchange of endblocks, which has range $\xi_o \ll R$ and magnitude equal to the number of potential bridges.

The attraction is independent of χ, since hydrophobes remain associated despite the freedom to sample other micellar cores. They estimated the number of chains in the gap between micelles as contact area/area per chain $= R\xi_o/\xi_o^2 = R/\xi_o = (p/4\pi)^{1/2}$, according to the Daoud−Cotton model, indicating a strong attraction for $p \gg 1$. Therefore, Semenov et al. anticipate a phase separation between a micellar gas and a condensed phase assumed to be volume-filling.

The application of this model to dilute micellar solutions of the associative triblocks of interest here is discussed thoroughly in a previous paper. In brief, we

Table 1. Measured and Predicted Micelle Properties[10]

	ODU	HDU
p	33 ± 9	20 ± 2
$[\eta]$ (m^3/kg)	0.051 ± 0.005	0.047 ± 0.003
R_H (nm) measured	21.2 ± 1.3	17.3 ± 0.4
R_H (nm) predicted	20.0	17.2
$1/\tau$	15 ± 4	11 ± 2

found the Daoud−Cotton model and the more sophisticated theory of Li and Witten to be equally successful in correlating intrinsic viscosities and hydrodynamic radii from dilute viscometry and dynamic light scattering. Coupling it with the adhesive hard sphere model to account for pair interactions enabled estimates of the attractive contribution to the virial coefficients, yielding the results in Table 1. The phase transition proved to be gas−liquid, rather than liquid−solid, as assumed by Semenov et al. Thus, we might expect the associated condensed phase to behave as a highly percolated fluid rather than a glassy solid.

Nonetheless the predictions of Semenov et al. for the viscoelasticity of the condensed phase are worth reviewing. The high-frequency modulus reflects the compression of the corona of closely packed micelles, with excluded volume interactions assumed to dominate the nonequilibrium stretching of bridging chains. This leads to three regimes: $\phi = 4\pi R^3 n/3p \approx 1$ with the micelles uncompressed and

$$R^3 G_\infty'/kT \approx p^{9/10} \tag{4}$$

$\phi > 1$ with weak compression and

$$R^3 G_\infty'/kT \approx p^{3/2}(\phi - 1)^2 \tag{5}$$

and $\phi \gg 1$ with a high degree of compression and

$$R^3 G_\infty'/kT \approx p^{3/2}\phi^{7/12} \tag{6}$$

The low shear viscosity follows from the modulus and the longer of two relaxation times, either the disengagement of the bridging chains λ or hopping of the micelles into free volume created by density fluctuations in the surroundings,

$$\lambda_{hop} = \frac{6\pi\mu R^3}{kT} \exp\left(\frac{4\pi R^3 G_\infty'}{3kT}\right) \tag{7}$$

The former is estimated to dominate for $\chi > p^{3/2}$, producing a low shear viscosity that increases monotonically with concentration and depends exponentially on χ. Otherwise, elastic hopping controls the relaxation, causing the low shear viscosity to pass through a maximum and then decrease with increasing concentration. This unusual behavior follows from the decrease in the elastic energy for creating the requisite free volume ($4\pi R^3 G_\infty'/3$) in the highly compressed limit in which the micellar radius shrinks from its dilute value due to screening in the polymer solution.

At this point, it is worth distinguishing among the various interaction energies influencing different aspects of the phenomena. The critical micelle concentration, the aggregation number, and the time scale for dissociation of a hydrophobe from a junction or micellar core depend on the difference in free energy of a hydrophobe in water and in the hydrophobic core of the micelle, i.e., χ. The attraction between micelles is insensitive to this hydrophobic energy but senses the difference in entropy of the hydrophobe plus the excluded volume and entropy of the soluble chain between looped and bridging configurations. This generates an equilibrium potential of mean force, or effective pair potential, between the micelles, in which the attraction is dominated by the entropy of the hydrophobe for highly stretched chains. The high-frequency modulus depends on the potential of the mean force for chains with hydrophobes that have insufficient time to exchange between micelles. Thus, it should depend on χ only through the aggregation number and micellar radius, whereas the viscosity is directly proportional to λ and increases exponentially with χ.

2.1. Materials and Methods. The associative polymers for our study were synthesized at Rohm and Haas as described previously.[10] These linear PEO chains, with molecular weight 35 kg/mol, polydispersity index 1.2, and endcaps of hexadecyl or octadecyl groups, are designated henceforth as hexadecyl unimer (HDU) or octadecyl unimer (ODU). The synthesis involved reacting the terminal hydroxyl groups of high molecular weight and narrow dispersity PEO with an excess of alkyl monoisocyanates in toluene to ensure complete termination with the hydrophobic alkanes. The product was purified by multiple precipitations in methanol and then recrystallized to remove any low-molecular-weight byproducts and residual reactants. Reverse-phase liquid chromatography and GPC confirmed all unimer chains to be fully endcapped with hydrophobes and to have the expected molecular weight. Thus, the final product has a homopolymer backbone with the same narrow molecular weight distribution as the PEO precursor and identical hydrophobes on the ends. Poly(ethylene oxide) (Fluka Chemicals) of 35 kg/mol molecular weight served, without further purification, as an unmodified, nonassociative analogue to HDU and ODU.

Polymer solutions were prepared with double-distilled deionized water containing 0−20 ppm hydroquinone as an oxidation inhibitor and stored at 4 °C, out of direct light, as further precaution against degradation. The associative polymer was allowed to hydrate with periodic shaking over a week to achieve full solubilization. All solutions were equilibrated at 25 °C before measurements.

A Rheometrics RFS II rheometer equipped with concentric cylinder (32 mm bob, 34 mm cup), 2.3° cone and plate (50 mm diameter), and parallel plate (50 mm diameter) geometries was used for steady shear and oscillatory measurements. Steady shear experiments had two modes. Shear sweeps at rates of 0.025−1000 s^{-1} with 2 min equilibration at each point yielded viscosity profiles for concentrations of 1.7−10 wt %. Phase separation prevented complete profiles at less than 1.5−1.7 wt %, but thoroughly mixing the solutions and quickly imposing a slow steady shear determined the Newtonian low shear plateau before the viscosity began decreasing due to the phase separation. Shear-induced phase separation is also observed for concentrations near the phase boundary, i.e., 1.7−2.5 wt %, as discussed later. Dynamic sweeps over strains of 0.2−100% at fixed frequencies defined the linear viscoelastic region and were followed by oscillatory measurements at frequencies of 0.01−200 rad/s and strain amplitudes of 2−20%. The smallest strain amplitude in the linear viscoelastic region producing a torque response within the transducer limits was selected.

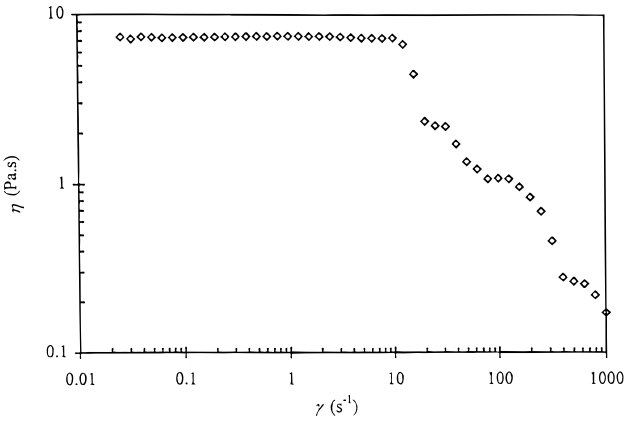

Figure 2. Steady shear viscosity of 2 wt % ODU.

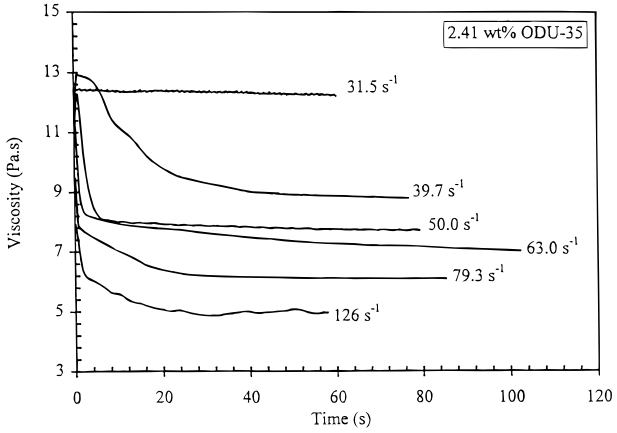

Figure 3. Variation with time of steady shear viscosity at fixed shear rates of 2.41 wt % ODU.

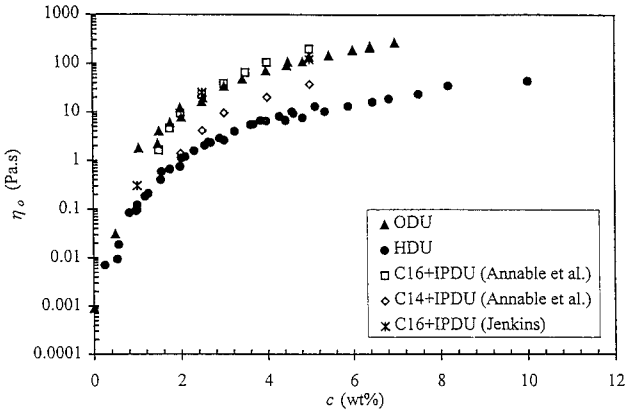

Figure 4. Low shear viscosity as function of concentration: HDU (●), ODU (▲), C_{16} + IPDU[7] (<>), and C_{16} + IPDU[6] (□).

3. Results

3.1. Steady Shear Viscosity. Steady shear viscosity profiles (Figure 2) obtained in the single-phase regime above 1.77 wt % for ODU and 1.56 wt % for HDU resemble those reported previously for the same class of hydrophobically endcapped PEO. Note the low shear plateau, very slight shear thickening, and shear thinning at high shear rates. However, there are some differences. The degree of shear thickening for ODU and HDU is much less than that observed by other groups.[5−7] Shear thinning, on the other hand, is much more abrupt, producing a steep, time-dependent change in viscosity that is accompanied by an abrupt decrease in the first normal stress difference, obtained from the force pushing the cone and plate apart. Furthermore, for $1.77 < c < 2.5$ wt %, the shear-thinning solution is not homogeneous, leaving a macroscopically inhomogeneous sample at the completion of the measurement. The abruptness of the shear-thinning regime differs significantly from the profiles previously reported by Annable et al.[7] and Jenkins et al.,[5,6] who attributed the thinning to a gradual breakdown of the associative network with increasing shear deformation, i.e., conversion from inter- to intramolecular association. The fluorescent spectroscopy of Richey et al.,[17] which found spectra and therefore aggregation numbers in pyrene-labeled associative solutions to be independent of shear rate, is consistent with this view.

For ODU and HDU, the sharp drop in viscosity and a correspondingly abrupt decrease in the normal stress suggest a more profound change in the associated solution. Measurements of the time dependence of the viscosity at fixed shear rates reveal time scales several orders of magnitude longer than those of the relaxation times of the associated network determined by oscillatory viscoelasticity (Figure 3). Note that at short times the viscosity at some shear rates even rises above the low shear limit, manifesting a modest but transient shear thickening. The slow decay cannot be due to a local rearrangement of the network structure or a fracture process but instead implies a shear-induced phase separation. Given that dilution leads to phase separation by rendering the favorable exchange of hydrophobes between micellar cores less likely, shearing at rates faster than the time scale for the exchange could well do the same. The corresponding time scale would be that of the macroscopic phase separation not that of the network breakdown. The behavior of the normal force appears consistent with this hypothesis, rising from essentially zero at low shear to a significantly positive value at the onset of shear thinning, as expected for an elastic liquid. A sharp reversal to small or slightly negative values in the shear-thinning region suggests relaxation of the chains, which would not be possible in a homogeneous solution. Additional support comes from visual observation of unusual patterns at high shear rates, e.g., rippling of the fluid surface in the Couette geometry or alternating concentric rings of dilute and condensed phases in the cone and plate geometry. In the latter geometry, the sample eventually flows radially out of the gap.

Viscoelastic surfactant solutions exhibit similar flow patterns of alternating turbid and clear rings in test geometries such as Couette, parallel plates, and cone and plate. Wheeler et al.[18] rationalized their observations as a consequence of coupling between the shear flow and concentration fluctuations that drive a phase transition. Our phenomenon appears similar, although we cannot confirm the details from our (stationary) visual observations after termination of shearing.

3.2. Low Shear Viscosity. Low shear viscosities, η_o, for homogeneous ODU and HDU solutions were extracted from the Newtonian plateaus, at steady state for single-phase samples or by transient measurements after mixing for samples in the two-phase region. Compared to the viscosities reported by Annable et al.[7] and Jenkins et al.[5,6] for similar molecular weights, our ODU corresponds to C_{16} + IPDU and HDU to a lesser degree to C_{14} + IPDU (Figure 4). The different coupling agents between the alkanes and the PEO backbone, isophorone diisocyanates for the C_{14} + IPDU and C_{16} +

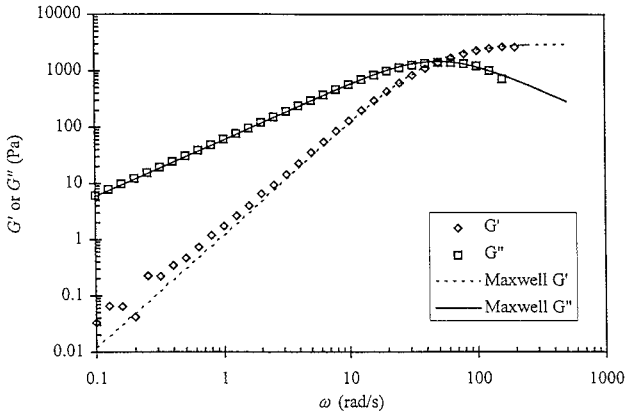

Figure 5. Storage modulus G' and loss modulus G'' of 4.5 wt % ODU. Lines represent fits of eqs 8 and 9 with $\lambda = 0.02$ s and $G_\infty' = 2950$ Pa.

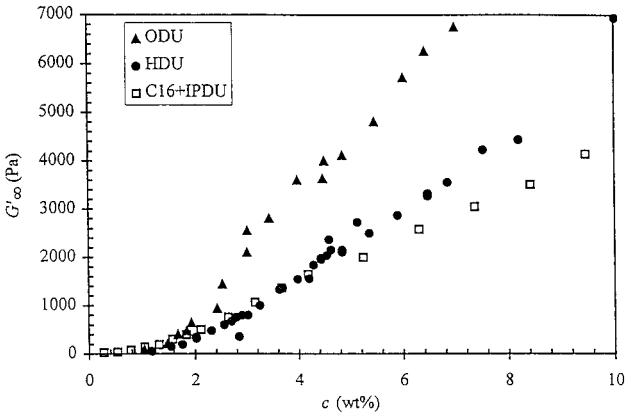

Figure 6. High-frequency modulus as function of polymer concentration: HDU (●), ODU (▲), C_{16} + IPDU[7] (□).

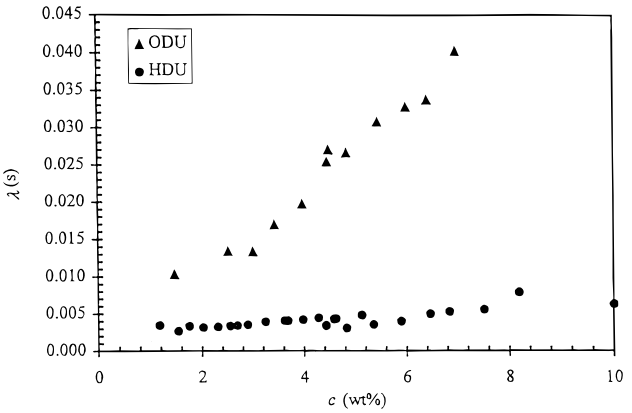

Figure 7. Relaxation time as function of polymer concentration: HDU (●) and ODU (▲).

IPDU and monoisocyanates for HDU and ODU, apparently compensate for the different hydrophobe sizes. Thus, the isophorone likely contributes the equivalent of two carbons to the overall hydrophobicity of the endgroup. At fixed backbone molecular weight, η_o depends strongly on hydrophobe size, as apparent at high concentration in Figure 4. Annable et al.[7] found the increase in η_o and λ with hydrophobe size to correspond to an association energy of ~0.9 kT per carbon unit, consistent with values for homologous series of ethoxylated nonionic surfactants.[19] Likewise, varying temperature reveals an Arrhenius dependence with a similar activation energy for η_o and λ.

Beyond the onset of aggregation at about 0.01 wt %,[2] the rapid rise of η_o with concentration results from the increasing probability of bridging between discrete micelles. The increase is roughly exponential for $c < 2$ wt %, although reproducibility is poorer for ODU than for HDU due to more rapid phase separation. For $c >$ 1.56−1.77 wt % the equilibrium condensed phase is fully percolated (Figure 1) but continues to gain in degree of association. At sufficiently high concentration, perhaps 5−10 wt %, the micelles become closely packed and fully associated. In the following sections, we will support this interpretation, in contrast to the more conventional explanations in terms of reptation of entangled chains[5] or network topology.[7]

3.3. Linear Viscoelasticity. Oscillatory shear responses of the associated solutions (Figure 5) suggest a simple viscoelastic fluid with a primarily viscous response at low frequency but a crossover at high frequency with a characteristic relaxation time λ. The storage G' and loss G'' moduli of ODU and HDU generally follow the single-relaxation Maxwell model

$$G'(\omega) = \frac{G_\infty'\omega^2\lambda^2}{1 + \omega^2\lambda^2} \tag{8}$$

$$G''(\omega) = \frac{G_\infty'\omega\lambda}{1 + \omega^2\lambda^2} \tag{9}$$

with frequency ω and high-frequency modulus G_∞'. The isothermal frequency scan reaches the expected power laws of 1 and 2 for G'' and G', respectively, at low frequencies and the crossover to a high-frequency plateau that identifies G_∞'. Sometimes temperature−time superposition as performed by Annable et al.[7] would be necessary to reveal the full plateau, but we fit instead to eqs 8 and 9.

For both HDU and ODU, G_∞' increases monotonically with concentration, with a more dramatic ascent for ODU (Figure 6). The dependence appears quadratic at low concentrations and linear at the upper end of the range. Although C_{16} + IPDU has a viscosity similar to that of ODU, the corresponding G_∞' corresponds to that of HDU at low concentrations and falls below even that at higher concentrations. This may reflect either a significant fraction of the chains that lack one or more hydrophobes or a lower aggregation number due to the slightly different structure of the hydrophobe.

The relaxation times increase roughly linearly with concentration (Figure 7) with $\lambda = 10-40$ ms for ODU and 3−8 ms for HDU for $c = 1-8$ wt %. These values are about half those reported for C_{16} + IPDU and C_{14} + IPDU, respectively, and have a weaker dependence on concentration. The difference between HDU and ODU is consistent with the exponential dependence on hydrophobe size in η_o. Furthermore, the linear viscoelasticity is consistent with the steady shear in that $\eta_o = \lambda G_\infty'(1 \pm 0.1)$. Next, we examine the concentration dependence of η_o and G_∞' more closely to clarify the mechanisms responsible.

4. Discussion

4.1. High-Frequency Modulus. In the transient network theory, all chains are assumed to be elastically active and to have a longer time scale λ for dissociation

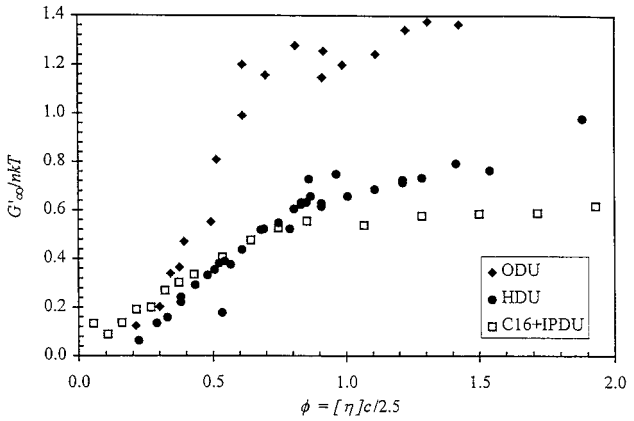

Figure 8. Transient network scaling for high-frequency modulus as function of volume fraction of micelles: HDU (●), ODU (▲), and C_{16} + IPDU[7] (□).

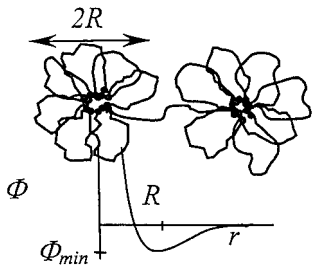

Figure 9. Intermicellar potential after Semenov et al.[12]

of the hydrophobe from a junction than for relaxation of the chain. Thus, the theory predicts $G_\infty'/nkT = 1$, although other authors and the data in Figure 8 show this not to hold for these associated solutions. Generally, G_∞'/nkT depends nonlinearly on concentration at the dilute end and, perhaps, approaches a constant at high concentrations. Annable et al.[7] attributed this to the changing topology of the network, particularly the transition from bridges to loops with dilution, and showed that G_∞'/nkT would approach unity if all chains form bridges and are elastically effective. Thus, their data for C_{16} + IPDU implies that up to 40% of the chains are incompletely capped with hydrophobes. However, such an argument does not account for the behavior of our ODU and HDU, which are 100% endcapped. The fact that scaling on nkT only accounts for the entropic elasticity of the chains, while G_∞'/nkT varies with hydrophobe size and exceeds unity for ODU, suggest that excluded volume interactions and the micellar structure may also be important, as argued by Semenov et al.[12]

In Figure 8, the concentration is expressed as the hydrodynamic volume fraction of micelles, $\phi = [\eta]c/2.5$, with the intrinsic viscosity $[\eta]$ obtained from capillary viscometry of dilute solutions (Table 1). The plot of G_∞'/nkT versus ϕ identifies two regimes that are key to understanding these micellar solutions. For low concentration, $\phi < 0.64-1.0$, the scaled modulus varies linearly with concentration, indicating that the modulus itself increases quadratically. This suggests pairwise interactions between flowerlike micelles with an interaction potential (Figure 9), as proposed by Semenov et al.[12] For $\phi > 0.64-1.0$, the scaled modulus tends to level off, but the asymptote depends on aggregation number and, therefore, does not conform to the reversible network model.

From the micellar point of view, the viscoelasticity should depend on both the entropy and excluded volume

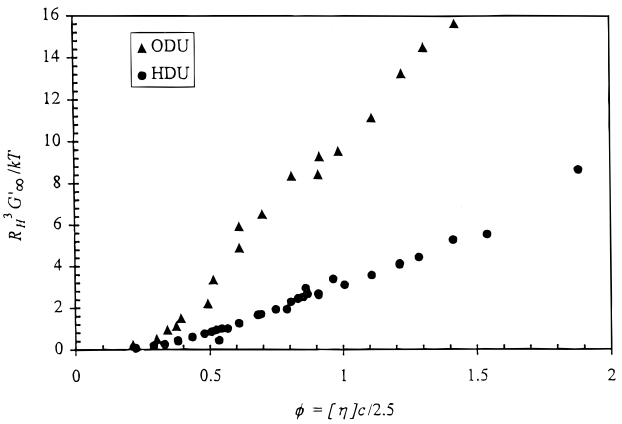

Figure 10. Colloidal scaling of high-frequency modulus as a function of volume fraction: HDU (●) and ODU (▲).

of the polymer chain, featuring a G_∞' that varies with micellar size, volume fraction, and aggregation number. We see that the modulus rises sharply for $0 < \phi < 0.64-1.0$ as first pairwise and then many-body interactions come into play, while for $0.64-1.0 > \phi$ the micelles become highly compressed and the modulus increases more slowly and, perhaps, linearly. While Semenov et al.[12] provide a sound physical picture of the micellar association, they focus primarily on $\phi > 0.64-1.0$. Since we observe a gas−liquid transition (Figure 1) rather than the gas−amorphous solid one they hypothesize, the modulus of the equilibrium fluid phase varies systematically with concentration from the liquid-phase boundary at $\phi = 0.30-0.40$ to close packing at $\phi = 0.64-1.00$. Simply rescaling ϕ on the observed value at the phase boundary would not represent the structure and interactions in the micellar solution accurately. For example, where they envision a volume-filling assembly of close-packed micelles at the phase boundary, we expect a moderately concentrated but highly percolated solution.

A more accurate picture is obtained by combining the expectations of Semenov et al.[12] for the intermicellar potential with the formalism developed for relating the modulus to pair potentials for colloidal dispersions.[20] From this point of view, G_∞' should scale with the thermal energy density kT/R_H^3 and depend on the volume fraction ϕ and the dimensionless interparticle force, motivating a plot of $R_H^3 G_\infty'/kT$ against ϕ (Figure 10). The roughly quadratic concentration dependence in the dilute regime indicates the importance of pairwise interactions; the prefactor is about 10 times the dilute limit for hard spheres ($0.202\phi^2$).

The modulus for these micellar solutions derives from an interaction potential Φ that includes compression of the corona and extension of bridging chains, rather than from the Brownian force that accounts for the modulus of hard spheres. From the colloidal theories without hydrodynamic interactions,

$$\frac{R^3 G_\infty'}{kT} \approx \phi^2 \int s^4 \frac{\mathrm{d}}{\mathrm{d}s}\left(\frac{\Phi}{kT}\right)\frac{\mathrm{d}g}{\mathrm{d}s}\,\mathrm{d}s \qquad (10)$$

with $s = r/R$ and $g(s)$ as the radial distribution function.[21] According to Semenov et al., the attraction scales as

$$\Phi/kT \approx -O(R/\xi_o) \qquad (11)$$

with a range that equals the outermost blob size ξ_o

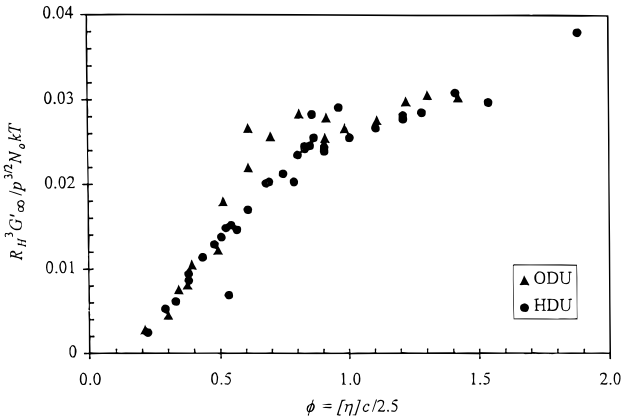

Figure 11. Correlation of high-frequency modulus according to eq 16: HDU (●) and ODU (▲).

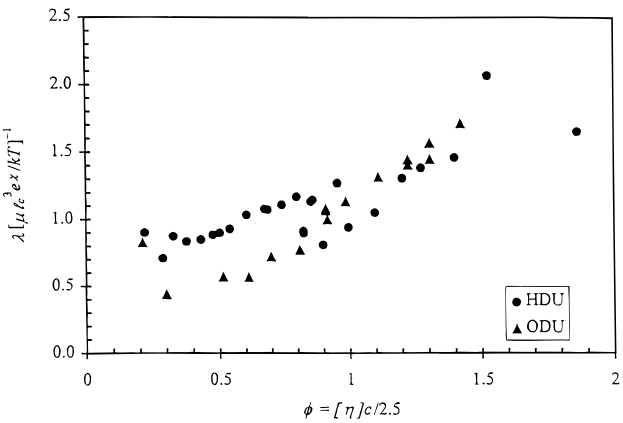

Figure 12. Scaled relaxation time as function of micelle volume fraction: HDU (●) and ODU (▲).

defined by the Daoud−Cotton model. Thus,

$$\frac{d\Phi/kT}{ds} \approx O\left(\frac{R}{\xi_o}\right)^2 \quad \text{and} \quad \frac{dg}{ds} \approx O\left(\frac{R}{\xi_o} g\right) \tag{12}$$

For a dilute dispersion of spheres with a short-range attraction and a relatively hard repulsion, the pair probability density is

$$g(s) = H(s - 2) + \delta(s - 2)/6\tau \tag{13}$$

where H is the Heaviside function and δ is the Kronecker function. Integrating $g(s)$ yields the number of nearest neighbors explicitly as

$$N_o = 3\phi \int [g(s) - 1] s^2 \, ds = 2\phi/\tau \tag{14}$$

Substituting eqs 13 and 15 into eq 10 indicates the magnitude of the modulus in the dilute limit to be

$$G_\infty' \approx kT(R/\xi_o)^3 \phi N_o / R^3 \tag{15}$$

with $R/\xi_o \approx p^{1/2}$ from the Daoud−Cotton model.

This analysis suggests replacing R with R_H and plotting

$$\frac{R_H^3 G_\infty'}{p^{3/2} N_o kT} \approx f(\phi) \tag{16}$$

with the values for R_H and p taken from dynamic light scattering and dilute viscometry and $1/\tau$ from dynamic light scattering and the phase behavior (Table 1). The scaling collapses the data for ODU and HDU rather nicely (Figure 11), supporting the argument that micellar structure, through the excluded volume and entropic attraction, determines the viscoelasticity of the associated solutions. The scaled modulus is not $O(1)$, perhaps because we have omitted prefactors and neglected hydrodynamic interactions. Although the analysis for good solvents and highly stretched chains absorbs the excluded volume parameter into R_H and ξ_o, our chains probably are not that extended. Thus, the curve may also depend on the excluded volume or Flory χ parameter and, therefore, may not be universal. A full theory would require an explicit expression for the pair potential as a function of micellar structure, the equilibrium radial distribution function over a wide concentration range, and hydrodynamic mobilities accounting for permeability of the corona to solvent.[20]

4.2. Relaxation Time. With G_∞' capturing the majority of the concentration dependence, $\lambda = \eta_o/G_\infty'$ should then account for the transient nature of the associations that control the relaxations with less sensitivity to concentration. The effects of temperature and hydrophobe size on rheological properties establish the exponential dependence of λ on the association energy via eq 3, but the relaxation process also requires diffusion of the hydrophobe away from the micellar core. Scaling the measured λ with the right-hand side of eq 3 should give a dimensionless relaxation time of $O(1)$ but does not if the diffusion length equals the end-to-end distance of the triblock. Only a much shorter length, such as the size of the hydrophobe or the hydrophobic core, accomplishes this. The diameter, $2R_c$, of the latter can be estimated from the bulk density ρ and molar mass m of the alkane chains as

$$2R_c = 2\left(\frac{3}{2\pi} \frac{pm}{\rho N_A}\right)^{1/3} \tag{16}$$

We obtain $2R_c = 3.34$ and 3.45 nm for HDU and ODU, respectively, which are consistent with the 2−5 nm estimated from fluorescence studies[4] and small-angle neutron and X-ray scattering.[22]

The dimensionless relaxation time

$$\lambda\left(\frac{8\mu R_c^3}{kT} e^{\chi}\right)^{-1} \tag{17}$$

is then roughly $O(1)$ over the range of concentrations studied for both unimers. To superimpose these curves (Figure 12), we chose $\chi \approx 0.86\ kT$ per alkane carbon, close to the 0.9−1 kT previously estimated by Annable et al.[7] Since χ should depend primarily on the hydrophobe size, the linear variation with concentration probably comes from the free diffusion time, i.e., the prefactor in eq 3. In view of the superposition of the two sets of data and the $O(1)$ magnitude of the scaled relaxation time, we conclude that the disengagement of the hydrophobes is controlled by diffusion of the alkane ends out of and away from the hydrophobic core with negligible effect on relaxation of the midblock.

5. Conclusions

Our purpose has been to demonstrate that the macroscopic properties of associative triblock copolymers can be interpreted in terms of the structure and interactions of flowerlike micelles. First, viewing the associative

micelles as adhesive hard spheres permits an estimate of the strength of the entropic attraction, which depends on hydrophobe size through the aggregation number. The attraction produces a gas−liquid-phase transition at low concentration, as well as enhancing the viscosity and viscoelasticity at high concentrations. Rheological properties reflect both the colloidal nature of micelles and the dynamics of the associated solution as controlled by the reversible bridging. By scaling G_∞' and λ and recognizing that $\eta_0 = \lambda G_\infty'$, we have related the rheology of the associated solution to the micellar structure, as represented by the aggregation number, the micellar radius, and the integral strength of the entropic attraction. At low concentrations, the rheology is dominated by pairwise interactions between the associating spherical micelles. As the micelles become closely packed at higher concentrations, the density of bridging chains increases and the behavior approaches the ideal transient network limit.

Acknowledgment. We thank Peter R. Sperry for sustained encouragement and advice in this undertaking and acknowledge financial support from the program in Particulate and Hydraulic Processes in the Division of Engineering of the National Science Foundation.

References and Notes

(1) Winnik, M. A.; Yekta, A. *Curr. Opin. Colloid Interface Sci.* **1997**, *2*, 424−436.
(2) Wang, Y.; Winnik, M. A. *Langmuir* **1990**, *6*, 1437−1439.
(3) Maechling-Strasser, C.; Clouet, F.; Francois, J. *Polymer* **1992**, *33*, 1021−1025.
(4) Yekta, A.; Xu, B.; Duhamel, J.; Adiwidjaja, H.; Winnik, M. A. *Macromolecules* **1995**, *28*, 956−966.
(5) Jenkins, R. D., Ph.D. Thesis, Lehigh University, Bethlehem, PA, 1990.
(6) Jenkins, R. D.; Silebi, C. A.; El-Aasser, M. S., *Polym. Mater. Sci. Eng.* **1989**, *61*, 629−633.
(7) Annable, T.; Buscall, R.; Ettelaie, R.; Whittlestone, D. *J. Rheol.* **1993**, *37*, 695−726.
(8) Walderhaug, H.; Hansen, F. K.; Abrahmsen, S.; Persson, K.; Stilbs, P. *J. Phys. Chem.* **1993**, *97*, 8336−8342.
(9) Kaczmarski, J. P.; Glass, J. E. *Macromolecules* **1993**, *26*, 5149−5156.
(10) Pham, Q. T.; Russel, W. B.; Thebeault, J. C.; Lau, W. *Macromolecules*, **1999**, *32*, 2996−3005.
(11) Daoud, M.; Cotton, J. P. *J. Phys.* **1982**, *43*, 531−538.
(12) Semenov, A. N.; Joanny, J.-F.; Khokhlov, A. R. *Macromolecules* **1995**, *28*, 1066−1075.
(13) Milner, S. T.; Witten, T. A. *Macromolecules* **1992**, *25*, 5495−5503.
(14) Green, M. S.; Tobolsky, A. V. *J. Chem. Phys.* **1946**, *14*, 80−92.
(15) Tanaka, F.; Edwards, S. F. *J. Non-Newtonian Fluid Mech.* **1992**, *43*, 247−309.
(16) Li, H.; Witten, T. A. *Macromolecules* **1994**, *27*, 449−457.
(17) Richey, B.; Kirk, A. B.; Eisenhart, E. K.; Fitzwater, S.; Hook, J. *J. Coatings Technol.* **1991**, *63*, 31−40.
(18) Wheeler, E. K.; Fischer, P.; Fuller, G. G. *J. Non-Newtonian Fluid Mech.* **1998**, *75*, 193−208.
(19) Vijayendran, B. R. *Polymer Colloids II*; Fitch, R. M., Ed.; Plenum Press: NY, 1980; pp 209−224.
(20) Elliott, S. L.; Russel, W. B. *J. Rheol.* **1998**, *42*, 361−378.
(21) Lionberger, R.; Russel, W. B. *J. Rheol.* **1994**, *38*, 1885−1908.
(22) Francois, J.; Maitre, S.; Rawiso, M.; Sarazin, D.; Beinert, G.; Isel, F. *Colloids Surfaces A* **1996**, *112*, 251−265.

MA990215X